ELSEVIER

Numerical investigation of natural convection in a vertical slot with two heat source elements

A. A. Dehghan
School of Mechanical Engineering, Yazd University, Yazd, Iran

M. Behnia
School of Mechanical and Manufacturing Engineering, The University of New South Wales, Sydney, Australia

Numerical modeling of natural convection air cooling of two heat-generating devices in an upright open-top slot has been considered. The heat sources are located on a vertical substrate of finite thermal conductivity, and the effect of different substrate material on the heat transfer performance has been quantified. The influence of the heat generation rate and the separation distance between the sources has been investigated. It has been shown that wall conduction is important, and for substrates with a finite thermal conductivity, it is essential that the conjugate analysis is employed.

Keywords: natural convection; open cavity; electronic cooling

Introduction

The reliability of electronic data-processing systems is a very important issue and depends on such parameters as semiconductor devices, packaging, and cooling systems. The thermal design of equipment and devices must ensure that component temperatures are maintained below a safe functional limit. This is primarily a reliability consideration. It has been found that various failure mechanisms are thermally activated, and failure rates increase rapidly with an increase in operating temperature (Doshy 1984). In addition, controlling the temperature variation from device to device in electronic equipment is important in order to reduce the level of thermal stresses so that the integrity of miniaturized circuits and electronic connections and the reliability of the packages themselves can be maintained. Different cooling schemes are available for maintaining the safe operating environment for semiconductor devices. The complexity of the cooling techniques applied to an electronic system depends on such factors as cost, operating environment, and available space. However, the key design parameters are the level of integration packaging technology and heat dissipation rate. Natural convection cooling has been and remains one of the promising techniques in thermal control of electronic systems. This method is intrinsically reliable, maintenance and noise free, and widely applicable in electronic systems employing low-heat-generating devices.

Many experimental and numerical studies have been performed in geometries containing multiple heat-generating devices in order to examine the capability of natural convection schemes. One of the first of these in which natural convection heat transfer from multiple heat sources was considered is the study of Jaluria (1982). In that study, multiple isoflux heat sources were mounted on an otherwise adiabatic vertical wall, and the boundary-layer form of the governing equations was employed. The effect of the heat source separation distance on the heat transfer coefficient of the downstream heat source was examined. The same geometry was considered in a later study of Jaluria (1985a), and the full governing equations were considered in order to examine the validity of the boundary-layer approximation. It was concluded that only for large values of Grashof number, the problem may be treated as a boundary-layer flow.

Milanez and Bergles (1986) carried out an experimental study to examine the effect of a wake which arises from a bottom heat source on the heat transfer performance of the upper component. Air and water were used, and the results were compared with the theoretical predictions of Jaluria (1982). Park and Bergles (1987) investigated the effect of a bottom heated element on the heat transfer rate of the upper one. An in-line array of two heaters was tested for a range of separation distances using R-113 as the cooling fluid. For all cases, the heat transfer coefficient of the upper heater was lower than that of the bottom one. This was contrary to the findings of Jaluria (1982) and Milanez and Bergles in which this ratio was found to be higher than unity for high separation distances. Keyhani et al. (1988a) experimentally investigated natural convection in a tall cavity heated by 11 equally spaced isoflux discrete heat sources mounted on an adiabatic vertical wall of the enclosure. The heat transfer coefficient generally decreased from the bottom heater to the top one. This was verified in their later study (Keyhani et al. 1988b).

Address reprint requests to Prof. M. Behnia, School of Mechanical and Manufacturing Engineering, The University of New South Wales, Sydney 2052, Australia.

Received 27 June 1995; accepted 29 March 1996

Int. J. Heat and Fluid Flow 17: 474–482, 1996

655 Avenue of the Americas, New York, NY 10010

0142-727X/96/$15.00
PII S0142-727X(96)00052-X

Afrid and Zebib (1989) considered natural convection air cooling of multiple heat-generating devices mounted on a vertical adiabatic wall. Components were allowed to have a finite thickness and thermal conductivity. Hence, conduction heat transfer in the components was included. For the case of equally spaced and powered components, the temperature increased from the lower component to the top one. They concluded that increasing the spacing between the components had a negligible influence on the bottom component temperature, while it marginally reduced the temperature of the upper components.

The thermal interaction of two heat sources mounted on an insulated flat plate was experimentally studied by Tewari and Jaluria (1990). The effects of plate orientation and heat source separation distance were examined for the pure natural convection, buoyancy dominated, and mixed convection regimes. For pure natural convection and a vertical plate orientation, the presence of the upstream heat source increased the temperature of the downstream one.

Close investigation of these studies reveals that in most of them, the vertical wall supporting the heat sources was adiabatic and interaction between the heat sources was only due to the thermal wakes of upstream sources. However, because most of these investigations are related to electronic cooling, and because printed circuit boards normally have a finite thermal conductivity, the devices can influence the heat transfer performances of each other through convection in the flow as well as conduction in the substrate. Most of the above-mentioned studies noted that the downstream heat source had no influence on the temperature of the upstream one, due to negligible diffusion of heat in the fluid, especially when boundary-layer approximation is employed. In a realistic situation, because conduction must be considered, this may not be true. The necessity of conjugate analysis under this circumstance is stated by Jaluria (1982, 1985b).

In the present investigation, natural convection air cooling of two heated strips, flush mounted on the left vertical wall of an open-top cavity is considered (Figure 1). The vertical walls of the cavity are assumed to be heat conductive. The nondimensional parameters of importance which affect the heat transfer performance are the Rayleigh number (Ra*), separation distance between the heat sources (l/s), and the ratio of the solid to the fluid thermal conductivity (k_r). These parameters are varied over a realistic range of interest and their effect on the heat transfer performance is quantified. However, it is noted that for all the simulations presented here, it is assumed that the slot has an aspect ratio (λ) of 5, wall thickness ratio (w_r) of 0.1 and the position of the upper heater (referred to as heat source 1) and the sizes of both heaters are fixed.

Analysis

Governing equations

The vorticity-stream function formulation of the two-dimensional (2-D) Navier–Stokes equations is used in the fluid region. Invoking the Boussinesq approximation, the governing equations are

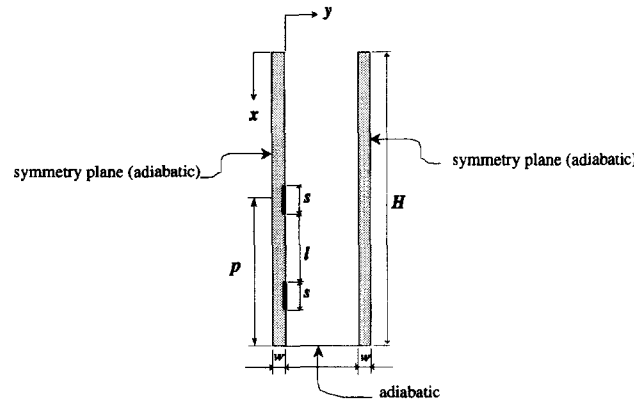

Figure 1 Schematic diagram of two heat sources in an open-top cavity

Notation

c_p fluid specific heat capacity
d cavity width
g acceleration attributable to gravity
H cavity height
k_r thermal conductivity ratio, k_s/k_f
l separation distance between the heat sources
n normal direction to the wall
p vertical position of the heat source
Pr Prandtl number, υ/α_f
q'' input heat flux (dimensional)
Ra* $\dfrac{g\beta q_1'' d^4}{k_f \upsilon^2}\dfrac{\mathrm{Pr}}{\lambda}$, Rayleigh number
s height of the heat source
t time
T temperature
U dimensionless velocity in the x direction, ud/α
V dimensionless velocity in the y direction, vd/α
w thickness of the walls
w_r wall thickness ratio, w/d
x, y coordinates
X, Y dimensionless coordinates ($X = x/d$, $Y = y/d$)

Greek

α thermal diffusivity
α_r thermal diffusivity ratio, α_s/α_f
β fluid coefficient of thermal expansion
θ dimensionless temperature, $(T - T_o)/(q_1'' d/k_f \lambda)$
λ aspect ratio, H/d
υ (kinematic viscosity)^2
ξ dimensionless vorticity
ρ density
τ $t\upsilon/d^2$
Ψ dimensionless stream function

Subscripts

1, 2 first (upper) and second (lower) heat source
f fluid
o ambient condition
s solid
w surface of the wall

written in nondimensional form as:

$$\frac{\partial \xi}{\partial \tau} + \frac{1}{\mathrm{Pr}}\left(U\frac{\partial \xi}{\partial X} + V\frac{\partial \xi}{\partial Y}\right) = \nabla^2 \xi + \mathrm{Ra}^* \frac{\partial \theta}{\partial Y} \tag{1}$$

$$\frac{\partial \theta}{\partial \tau} + \frac{1}{\mathrm{Pr}}\left(U\frac{\partial \theta}{\partial X} + V\frac{\partial \theta}{\partial Y}\right) = \frac{1}{\mathrm{Pr}}\nabla^2 \theta \tag{2}$$

$$\nabla^2 \Psi + \xi = 0 \tag{3}$$

in which Ψ, the stream function and ξ, the vorticity are defined by

$$U = \frac{\partial \Psi}{\partial Y} \quad \text{and} \quad V = -\frac{\partial \Psi}{\partial X} \tag{4}$$

$$\xi = \frac{\partial V}{\partial X} - \frac{\partial U}{\partial Y} \tag{5}$$

In the vertical conductive walls, the following one-dimensional (1-D) conduction equation is used:

$$\frac{\mathrm{Pr}}{\alpha_r}\frac{\partial \theta_s}{\partial \tau} = \frac{\partial^2 \theta_s}{\partial X^2} + Q_{\mathrm{con}} \tag{6}$$

in which

$$Q_{\mathrm{con}} = \frac{1}{k_r w_r}\left[\lambda + \left(\frac{\partial \theta}{\partial n}\right)_f\right] \qquad \text{on the heat source surface}$$

and

$$Q_{\mathrm{con}} = \frac{1}{k_r w_r}\frac{\partial \theta}{\partial n_f} \qquad \text{on the unheated surfaces}$$

The local Nusselt number $\mathrm{Nu}(X)$ is used to express the rate of convective heat transfer at any position on the vertical walls:

$$\mathrm{Nu}(X) = -\frac{1}{\theta_w}\left(\frac{\partial \theta_f}{\partial n}\right)_w \tag{7}$$

Boundary conditions

The outside of each vertical wall is assumed to be a symmetry plane (i.e., adiabatic). An energy balance for an element of each of the vertical walls yields the appropriate equations coupling the temperature in the fluid to that in the solid (Equation 6). All the solid boundaries of the cavity are assumed to be impermeable and nonslip, so that both Ψ and the fluid velocities are set to zero on these surfaces.

The computational domain is restricted to the cavity for both economy and simplicity. Therefore, appropriate boundary conditions are required for the open top. Here it is assumed that the incoming flow is at the ambient temperature, and the outgoing flow is assumed to have zero axial temperature gradient. For the case of a single heat source mounted on a vertical wall, Jaluria (1985a) has shown that the flow is a boundary-layer type. This is a valid assumption at a downstream location from the heat source, especially for higher Grashof numbers. Therefore, the horizontal component of the velocity V is assumed to be zero at the open boundary. The boundary condition for the vertical velocity U is obtained from the continuity equation which gives $\partial U/\partial X = 0$.

Similar approximate boundary conditions have been successfully used by Gosman et al. (1971) and Chan and Tien (1985) in their studies. Chan and Tien also showed that even for square cavities at moderate to high Rayleigh numbers, the flow and heat transfer were identical with those obtained from extending the computational domain outside the cavities. Abib and Jaluria (1988) employed the same boundary conditions for predicting buoyancy-driven flow generated by a discrete isothermal heat source inside a partially open enclosure. More recently, Lage et al. (1992) and Jones and Cai (1993) in their numerical study of natural convection heat transfer in open top cavities employed the same boundary conditions used here.

Computational procedure

Because the steady-state solution is of primary importance in this study, a false transient technique is employed for solving Equations 1–3. In this method, a pseudotransient time derivative is added to the right-hand side of Equation 3, and each equation is marched in time with a different time step. This allows a considerable saving in the computational effort. The governing flow Equations 1, 2, and 3 and the solid conduction Equation 6 are approximated by finite differences. First-order finite differences in time and second-order central differences in space are employed. The resulting finite difference form of the governing flow equations are solved by an ADI scheme, and a fully implicit scheme is employed for the conduction Equation 6.

Results

The results are divided into three main sections. In the first section, the effect of Ra* or input heat flux to the heat sources is investigated. In the second part, the conductivity of the side walls is varied, and its influence on the flow and thermal fields is examined. Finally, in the last section, attention is focused on the influence of the separation distance between the two heat sources on the flow and thermal fields and especially on heat transfer characteristic of the upper heat source. The influence of the heat flux ratio (q_2''/q_1'') is also evaluated for different values of k_r; however, the results are not presented here because of space limitation.

Uniform grids of 101×31, 101×41, and 101×51 were examined. The difference between predicted heat source Nusselt number for 101×31 and 101×41 grids was 1.56%; while this reduces to 0.88% for 101×41 and 101×51 grids. Therefore, a uniform 101×41 mesh was used in all the computations. The calculations were performed on an IBM RS/6000-320 workstation with typical requirement of 100 CPU seconds per 1000 iterations, with approximately 10^6 iterations being required to obtain a steady-state solution. The run time can be shortened by using the converged solution of a previously computed similar case as a starting solution. For some cases, different initial conditions were employed in order to evaluate if the final steady-state solution is sensitive to the choice of starting solution. A maximum error of 0.8% was observed between all dependent parameters. Therefore, it was assured that the final steady-state solution is independent of starting solution. However, a bad choice of starting solution may result in the divergence of the solution scheme.

Effect of input heat flux to the heat sources

In this section, the imposed heat fluxes on the heaters are assumed to be the same. They are varied from 50 to 1000 W/m^2 corresponding to the variation of Rayleigh number from 5.74×10^3 to 1.148×10^5. The nondimensional separation distance (l/s) is also assumed to be 2.2. Two values of k_r are selected here which represent cavities with adiabatic vertical walls (i.e., $k_r = 0$) and bakelite substrate (i.e., $k_r = 8.8$).

In Figure 2, the ratio of the temperature of the upper heater to the lower heater (referred to as heat source 2) and their Nusselt number ratios are presented as a function of Ra* for $k_r = 0$. It is clear that for all input fluxes and for the selected separation distance, the upper heat source has a higher temperature and a lower Nu than the lower heater. However, these differences diminish and approach their asymptotic values as Ra* is increased. Therefore, at low values of Ra*, the influence of the lower heater on the upper source is stronger. The temperature profiles over the left wall are shown in Figure 3 for two values of Ra* and k_r. At a fixed input heat flux or Ra*, the variation of the temperature is more pronounced along the wall, especially at the heat source locations for the cavity with adiabatic vertical walls. For $k_r = 0$, the maximum temperatures are at the trailing edges of the heaters; whereas, for $k_r = 8.8$, they shift toward the centre of the heaters. A noticeable reduction in the maximum temperature is observed for the case of the conductive wall, particularly for lower Ra*. However, the temperatures at locations downstream of the upper heater are the same for both $k_r = 0$ and 8.8.

Recently, an approximate method has been proposed by Lee and Yovanovich (1992) for determining temperature distribution in laminar free convection along a vertical plate with an arbitrary specified surface heat flux. It is noted that in their analysis, unlike ours, the bottom was not blocked. Their method is based on the linearization of the nonlinear laminar boundary-layer equations and decoupling of the temperature field from the flow field. In the present analysis, for high values of Ra*, a thin thermal boundary layer is formed along the left vertical wall. Comparison of the temperature distribution for $Ra^* = 6.88 \times 10^4$ and $k_r = 0$ with the analytical prediction of Lee and Yovanovich in Figure 4 shows good agreement. However, the temperature drops at the trailing edge of the heaters are less severe in this analysis than the approximate method. This is due to the shrouding effect of the right wall and the full governing equations solution which is employed in this analysis. As experimental or numerical data for this particular geometry is rare, comparisons have been made with what has been available. For the single heat source condition, comparisons have been made between the experimental observations and numerical results (Dehghan and Behnia 1996).

Influence of wall thermal conductivity

In this section, the effects of thermal conductivity of the vertical walls are examined for various values of the separation distance between the heat sources. The input heat flux to both heat sources is assumed to be the same and equal to 1000 W/m^2, corresponding to $Ra^* = 1.148 \times 10^5$. A broad range of thermal conductivity ratio is selected. This range covers the limiting case of the cavity with adiabatic vertical walls (i.e., $k_r = 0$) to the cavity with highly conductive walls (e.g., copper, $k_r = 1375$). For each value of k_r, the nondimensional separation distance (l/s) is varied from 0.6 to 3.4.

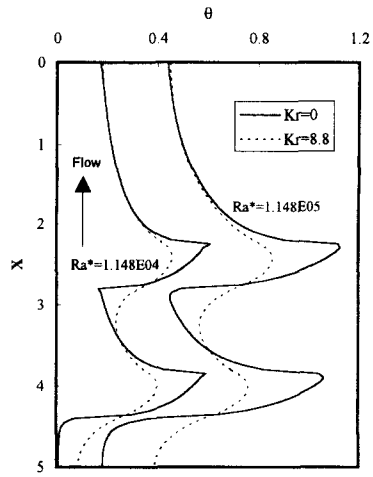

Figure 3 Temperatures distribution over the left wall for different values of k_r and Ra* [$q_1'' = q_2''$, and $l/s = 2.2$]

The flow and thermal fields are presented in Figure 5 for different values of k_r and for $l/s = 2.2$. No noticeable differences are observed in the flow fields except that the flow penetrates deeper inside the cavity for higher k_r. However, appreciable changes in the isotherms patterns are observed. For $k_r = 0$, the onset of the thermal boundary layer is at the leading edge of the second heat source, while this point moves toward the bottom of the cavity as k_r is increased. Isotherms are highly concentrated around the heaters for $k_r = 0$ and 8.8. The concentration of the isotherms on the proximity of the heat sources diminishes as k_r is increased. For high conductivity ratio, the isotherms are concentrated at the bottom location of the left wall instead of the heater location. This indicates a higher heat transfer rate at this location.

The fluid temperature distributions across the cavity at the centre of both heat sources are shown in Figures 6 and 7 for different values of k_r. Noticeable changes in the fluid temperature distribution are seen in these figures as k_r is increased. The

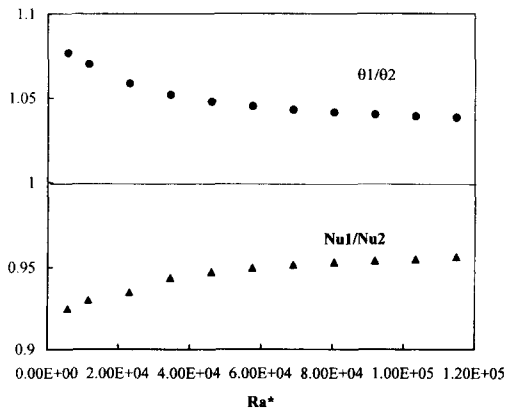

Figure 2 Variation of the ratio of the average temperature and Nusselt number of the upper source to the lower one as a function of Ra* [$q_1'' = q_2''$, $l/s = 2.2$, and $k_r = 0$]

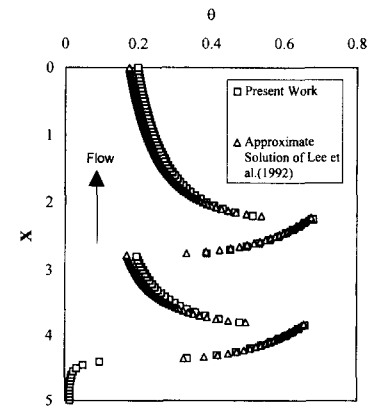

Figure 4 Temperature distribution along the left wall containing two heat sources for $Ra^* = 6.88 \times 10^4$, $k_r = 0$, and $l/s = 2.2$

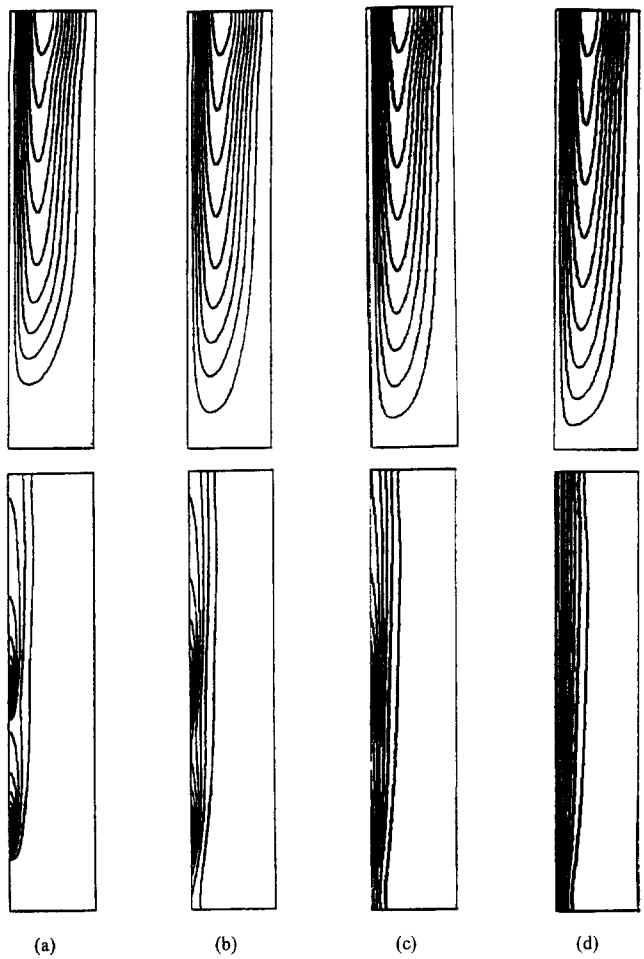

Figure 5 Streamlines and isotherms for $Ra^* = 1.148 \times 10^5$ and $l/s = 2.2$ for different values of k_r [(a) 0, (b) 8.8, (c) 29.7, (d) 1375]

temperature of the rising plume is lower at both heater locations for higher k_r due to both conduction in the wall and higher entrainment of the downward cold flow. The temperature gradients in the fluid also reduce with increasing k_r at both heater locations, resulting in lower convective heat fluxes. The lower concentration of isotherms around the heat sources for higher values of k_r also indicates the reduction in the temperature gradients in proximity of the heat sources, as seen in Figure 5.

The temperature distributions along the left wall containing the heat sources are illustrated in Figure 8 at $Ra^* = 1.148 \times 10^5$

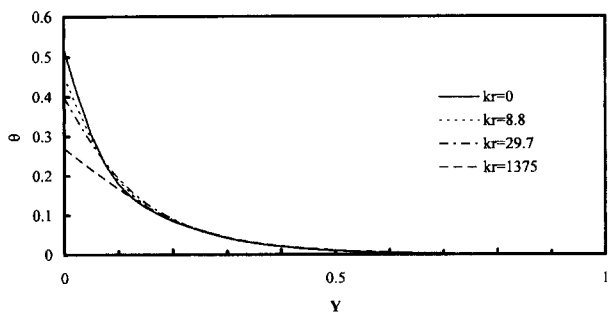

Figure 6 Comparison of the fluid temperature distribution at the middle of the upper heat source for different values of k_r [$Ra^* = 1.148 \times 10^5$, $q_1'' = q_2''$, and $l/s = 2.2$]

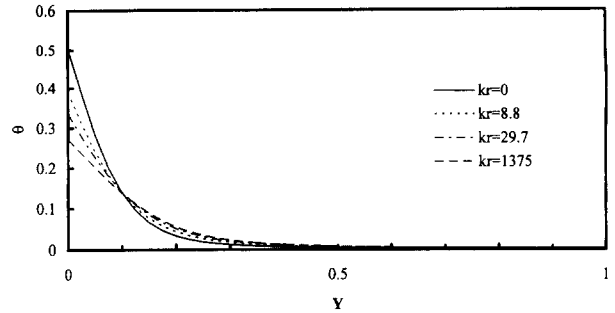

Figure 7 Comparison of the fluid temperature distribution at the middle of the lower heat source for different values of k_r

and $l/s = 2.2$ for various values of thermal conductivity ratio. Starting at the bottom of the wall (i.e., $X = 5$) for $k_r = 0$, the temperature is almost zero. By approaching the upstream heat source, the temperature increases slightly because of diffusion in the air. Near the leading edge of the upstream heat source, the temperature increases rapidly and reaches its first local maximum at the trailing edge of the upstream heater. From the trailing edge of this heat source to the leading edge of the downstream heat source, which is an adiabatic segment with the length of l, the temperature decreases sharply and then increases rapidly after the leading edge of the upper heater and reaches its second local maximum point. After that, it decreases continuously up to the top of the wall. It is noted that increasing k_r mitigates these variations. A noticeable decrease in the peak temperatures of the heat sources is seen with a considerable increase in the temperature of the upstream region of the second heat source (i.e., $4.5 < X < 5$) when k_r is increased. For $k_r = 0$, the decrease in the temperature of the wall after the downstream heat source is sharp, due to entrainment of the cold fluid into the rising plume when it passes the downstream heater. However, for the conductive wall, the decrease in the wall temperature downstream of the first heater is less pronounced. This is due to the fact that the cooling effect of the cold flow entrainment is partially compensated by conduction of the heat in the wall. For highly conductive walls, the temperature distribution is almost uniform. It is interesting to note that the difference between the maximum temperatures of the heaters is increased by increasing k_r up to approximately $k_r = 30$ and then decreases for higher values of k_r. Increasing k_r also leads to a shift in the maximum temperature locations from the trailing edges of the heaters

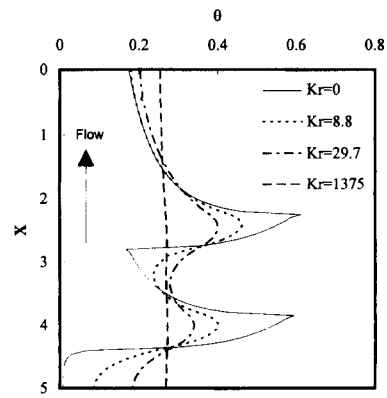

Figure 8 Comparison of the local temperature distributions over the left wall for different values of k_r [$Ra^* = 1.148 \times 10^5$, $q_1'' = q_2''$, and $l/s = 2.2$]

toward the centre. Furthermore, temperature changes become smooth over the heaters by increasing k_r, leading to a reduction in the difference between the maximum and average temperature of both sources.

For the case of the adiabatic walls, the interaction between the heat sources is due to the thermal wake of the upstream heater. In this case, the influence of the upper heater on the lower one is negligible. However, for the case of conductive walls, the lower heater influences the upper one through both its thermal wake and conduction in the wall. In addition, the upper heater also influences the lower heater via conduction in the wall. The degree of interaction through either the thermal wake or the conductive wall depends on the value of the thermal conductivity ratio. For low k_r, their interaction through the rising fluid is dominant, while for higher k_r, the interaction by conduction in the wall becomes more pronounced. It is seen that even for the low conductivity wall, the temperature distribution changes appreciably. For instance, for $k_r = 8.8$ and 29.7, the maximum temperature of the lower heater is 68 and 57% of the corresponding value for $k_r = 0$. For the downstream heater, these values are 76.5 and 65% of the corresponding values for $k_r = 0$. Therefore, using a simple adiabatic boundary condition may result in substantially different and sometime erroneous heat transfer data.

Figure 9 shows the effect of k_r on the nondimensional convective heat transfer coefficient of both heat sources. It is seen that an appreciable reduction in Nu occurs when k_r is increased up to the order of 100, after which the changes become gradual. Initial reduction of Nu is due to the contribution of the vertical wall in spreading the thermal energy generated at the heat source locations, leading to the reduction in contribution of convection to the fluid at these locations. For high conductivity, the wall effectively becomes isothermal, so further increase of k_r yields only marginal changes in heat transfer. For all cases, the lower heater has a higher convective heat transfer coefficient. Increasing k_r yields a thickening of the thermal boundary layer at the upper heat source. Also, for sufficiently high k_r, there is a continuous reduction in Nu from the bottom location of the wall to the top. Hence, the convective heat transfer is much higher at the bottom heat source than the top one.

Influences of heater separation distance

One of the interesting parameters in the thermal design of electronic systems is the proper placement of the heat-generating elements on the printed circuit boards in order to produce compact and thermally efficient equipment. In this section, the distance between the heat sources is varied, and the effect of the separation distance on the flow and thermal fields—in particular on heat transfer of the upper heaters—is examined.

In Figures 10 and 11, the streamlines and isotherms are presented for two different values of k_r and for various l/s. For

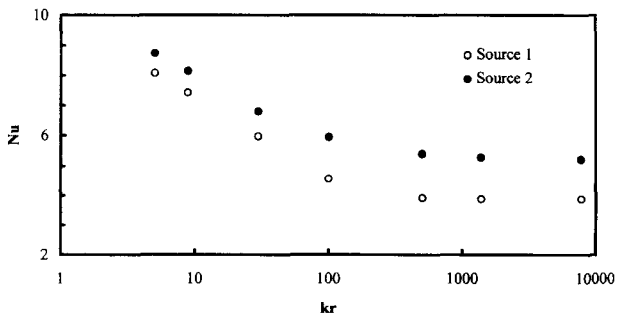

Figure 9 Influence of k_r on the average Nu of the lower and upper sources [$Ra^* = 1.148 \times 10^5$, $q_1'' = q_2''$, and $l/s = 2.2$]

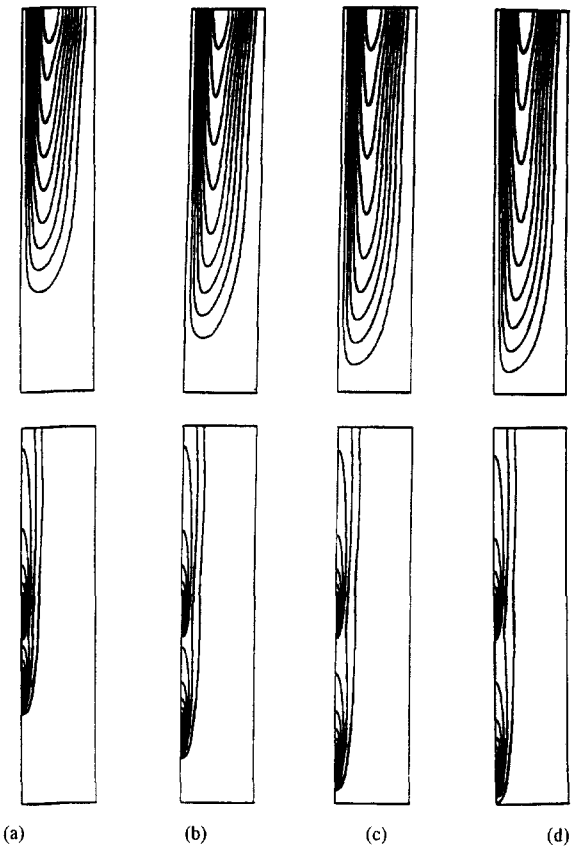

Figure 10 Streamlines and isotherms for $Ra^* = 1.145 \times 10^5$, $k_r = 0$ and different values of l/s [(a) 1, (b) 2.2, (c) 3, (d) 3.2]

both values of k_r, increasing l/s causes deeper penetration of the incoming flow inside the cavity. This is more pronounced for $k_r = 0$. Also for $k_r = 0$, the thermal boundary layers generated at the location of the two heat sources appear to be independent of each other for a sufficiently large value of l/s. For $k_r = 8.8$, the onset of the thermal boundary layer is at the bottom of the cavity for $l/s > 1$.

The effect of the separation distance on the flow and thermal fields is quantitatively shown in Figures 12 and 13 where the velocity and temperature profiles at the middle of the upper heat source are presented for various values of l/s. Increasing l/s increases the velocities at the middle of the upper heater for both values of conductivity ratio, as can be seen in Figures 12a and 12b. However, the increase in the velocities is higher for $k_r = 0$ due to a larger buoyancy of the flow. Negligible changes in velocities at the bottom heat source were observed as l/s was changed for $k_r = 0$. However, for $k_r = 8.8$, lower velocities at the location of the lower heater was seen as l/s was increased due to the smaller heat transfer area between the lower heat source and the bottom of the vertical wall. It is also noticed that for both conductivity ratios, increasing l/s increases the mass flow rate of the incoming cold flow. This, along with the increase in the velocities at the upper heater, enhances the convective heat transfer in the vicinity of that heat source. The temperatures are reduced at the upper heat source location as l/s is increased for both values of k_r (see Figures 13a and 13b). This is due to the entrainment of the cold fluid. Hence, as l/s is increased, the upper heater is exposed to a higher velocity and a lower temperature, resulting in an increase in the convective heat transfer coefficient.

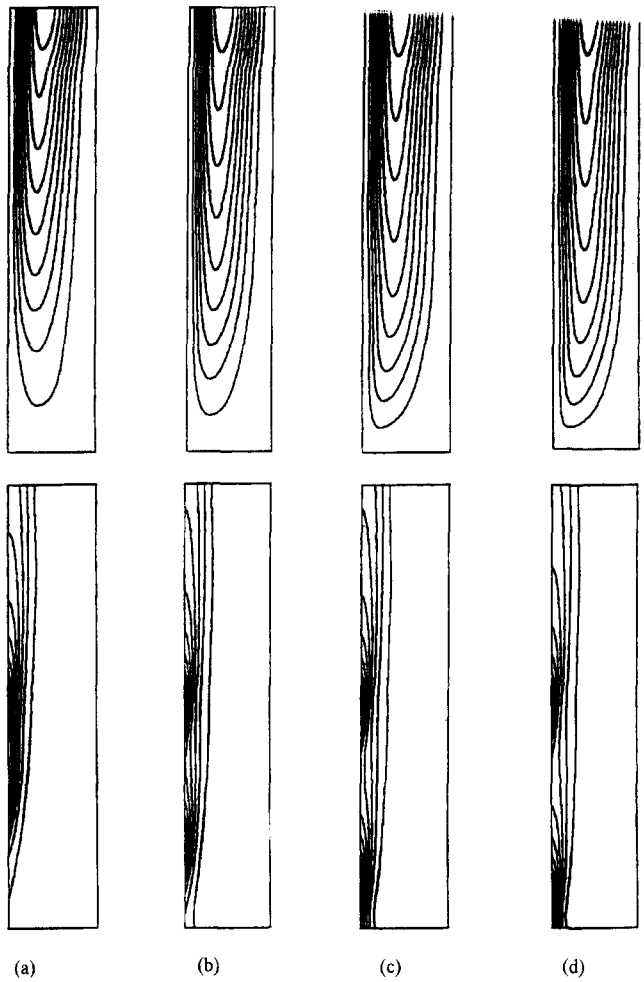

Figure 11 Streamlines and isotherms for $Ra^* = 1.145 \times 10^5$, $k_r = 8.8$ and different values of l/s [(a) 1, (b) 2.2, (c) 3, (d) 3.4]

The dependence of the heat transfer coefficient of the upper element on the separation distance for the case of $k_r = 0$ is shown in Figure 14. In this figure, the nondimensional heat transfer coefficient of the upper source (Nu_1) is normalized by the corresponding value for the lower source (Nu_2). The experimental data of Milanez and Bergles (1986) for a vertical adiabatic flat plate with two isoflux heated strips are also presented. The sharp increase in this ratio for l/s greater than three is due to a drop in Nu_2 as it approaches the bottom of the cavity.

The variations of the local temperature along the left wall for various l/s are shown in Figures 15, 16 for $k_r = 0$ and 8.8. In Figure 15, it is seen that increasing l/s reduces the temperature on the upper heat source. For $l/s > 3.2$, the temperature distribution over the upper heater is the same as if there was no upstream heater. However, the effect of the upper heater on the lower one is negligible, because no changes are observed in the temperature distribution of the lower heat source as l/s is increased or decreased. The only change in the lower heater temperature profile is due to the bottom adiabatic boundary when this heater is positioned right above it (i.e., $l/s = 3.4$). For the case of the cavity with conductive walls, the temperature of the upper heater is also reduced when the lower heater is moved downward (i.e., as l/s is increased). This is due to both reduction in the influence of the thermal wake of the lower heater and

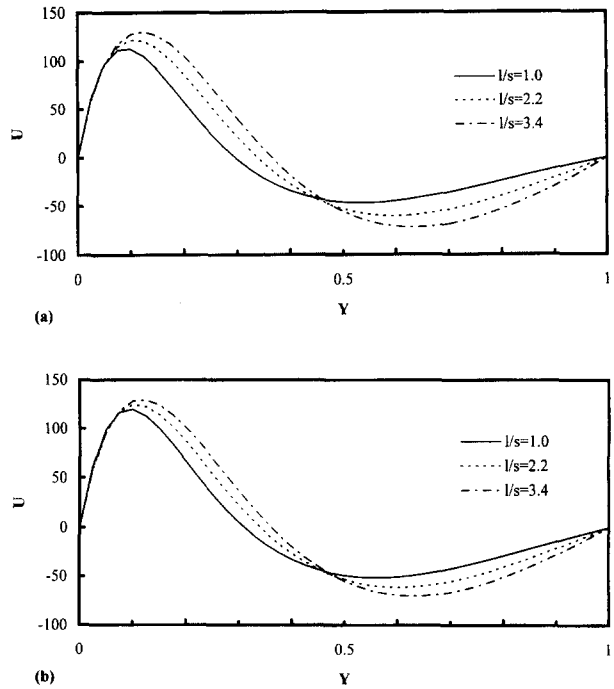

Figure 12 Vertical velocity profiles at the middle of upper heat source for various separation distances, $Ra^* = 1.148 \times 10^5$ and $q_1'' = q_2''$ [(a) $k_r = 0$ and (b) $k_r = 8.8$]

conduction in the vertical wall. However, it is seen that for conductive walls, both heaters are affected when l/s is increased or decreased. This is a result of the mutual interaction between the heaters, via conduction in the substrate, for the case of conductive walls.

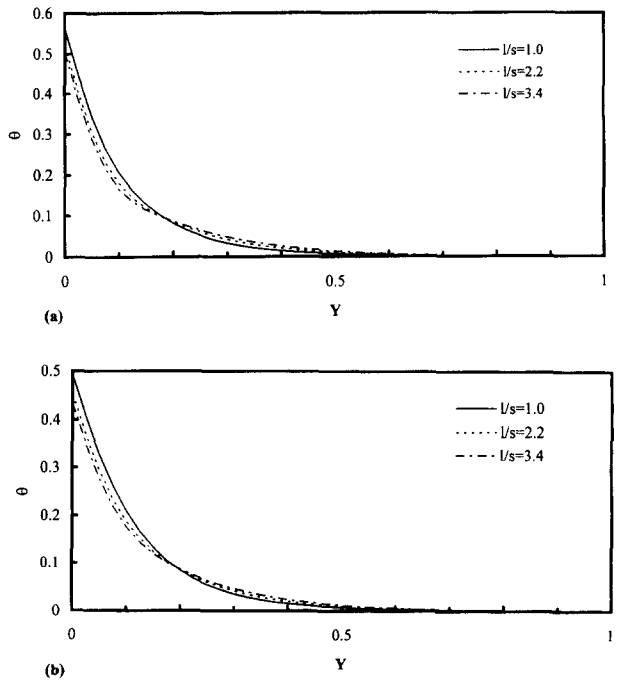

Figure 13 Fluid temperature distributions at the middle of the upper heat source for various separation distances, $Ra^* = 1.148 \times 10^5$ and $q_1'' = q_2''$ [(a) $k_r = 0$ and (b) $k_r = 8.8$]

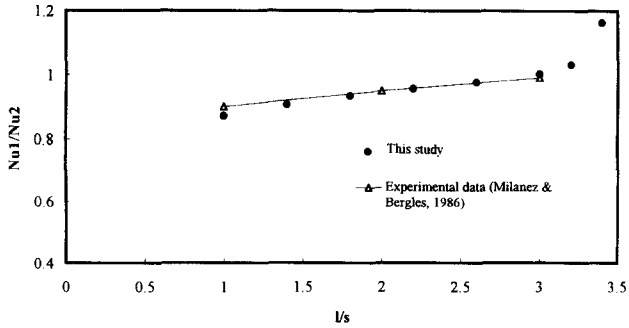

Figure 14 Variation of the ratio of the heat source Nu ($Ra^* = 1.148 \times 10^5$, $q_1'' = q_2''$, and $k_r = 0$)

Conclusions

Natural convection air cooling of two heat-generating devices mounted on a vertical wall of an upright open-top slot has been investigated numerically. This geometry models two electronic components placed on a printed wiring board (substrate). The influence of such design parameters as the heat generation rate, the separation distance between the heat sources, and the thermal conductivity of the vertical substrates were investigated. It was seen that the thermal interference between the heat sources was reduced when Ra* is increased. It was also observed that increasing l/s resulted an increase in velocities at the upper heat source for both conductive and adiabatic boundary conditions. This led to an enhancement in convective cooling of the upper located electronic component. A higher mass flow rate of cold flow entering the cavity was achieved when l/s was increased, which resulted in an increase in convection heat transfer from both components. However, it was found that the influence of the lower heat source on the upper one was negligible for $l/s > 3$ regardless of the wall thermal conductivity. Hence, this spacing distance may be considered as an optimal spacing in order to keep compactness of the electronic system in this specific configuration. It was also shown that for the case of adiabatic walls, the upstream component was not affected when l/s was changed. For the conductive walls, both heaters were affected by varying l/s. For substrates with sufficiently high thermal conductivity, the movement of the upstream heat source had no effect on the convective heat transfer rate of the downstream one; whereas, for low conductivity this effect was noticeable.

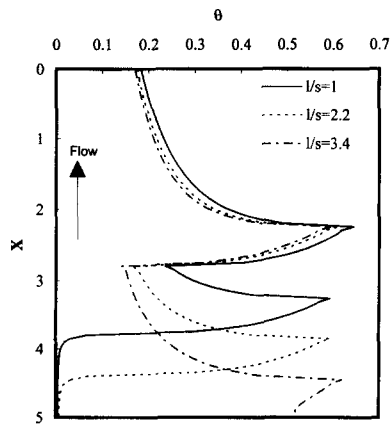

Figure 15 Local temperature distributions along the left wall for various values of separation distance ($Ra^* = 1.148 \times 10^5$, $q_1'' = q_2''$, and $k_r = 0$)

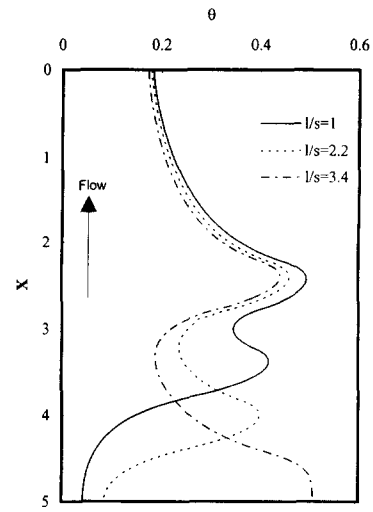

Figure 16 Local temperature distributions along the left wall for various values of separation distance ($Ra^* = 1.148 \times 10^5$, $q_1'' = q_2''$, and $k_r = 8.8$)

For adiabatic substrates, the upper source had no influence in the thermal characteristics of the lower one. However, for cavities with conductive walls, there was mutual thermal interaction between the sources, and the upper heater was influenced by the presence of the lower one due to both conduction in the wall and thermal wake generated by the lower heater.

The thermal performance of a heat generating component in the thermal wake of another lower located component was also investigated. The presence of such a heat source causes a stronger flow in the cavity for both adiabatic or conductive boundaries. For substrates with a finite thermal conductivity it is essential that the conjugate analysis is employed.

References

Abib, A. H. and Jaluria, Y. 1988. Numerical simulation of the buoyancy-induced flow in a partially open enclosure. *Num. Heat Transfer*, **14**, 235–254

Afrid, A. and Zebib, A. 1989. Natural convection air cooling of heated components mounted on a vertical wall. *Num. Heat Transfer*, **15**, 243–259

Chan, Y. L. and Tien, C. L. 1985. A numerical study of two-dimensional laminar natural convection in shallow open cavities. *Int. J. Heat Mass Transfer*, **28**, 603–612

Dehghan, A. A. and Behnia, M. 1996. Combined natural convection, conduction and radiation heat transfer in a discretely heated open cavity. *J. Heat Transfer*, **118**, 56–64

Doshy, I. 1984. Reliability impact of thermal design. *Technical Conference—IEPS, 4th Annual International Electronic Packaging Conference*, 307–317

Gosman, A. D., Lockwood, F. C. and Tatchell, G. 1971. A numerical study of the heat-transfer performance of the open thermosyphon. *Int. J. Heat Mass Transfer*, **14**, 1717–1730

Jaluria, Y. 1982. Buoyancy-induced flow due to isolated thermal sources on a vertical surface. *J. Heat Transfer*, **104**, 223–227

Jaluria, Y. 1985a. Interaction of natural convection wakes arising from thermal sources on a vertical surface. *J. Heat Transfer*, **107**, 883–892

Jaluria, Y. 1985b. Natural convection cooling of electronic equipment. In *Natural Convection, Fundamentals and Applications*, S. Kakac, W. Aung, and R. Viskanta, (eds.), 961–987

Jones, G. F. and Cai, J. 1993. Analysis of a transient asymmetrically heated/cooled open thermosyphon. *J. Heat Transfer*, **115**, 621–630

Keyhani, M., Prasad, V. and Cox, R. 1988a. An experimental study of natural convection in a vertical cavity with discrete heat sources. *J. Heat Transfer*, **110**, 616–624

Keyhani, M., Prasad, V., Shen, R. and Wong, T. T. 1988b. Free convection heat transfer from discrete heat sources in a vertical cavity. In *Natural and Mixed Convection in Electronic Equipment Cooling*, R. A. Writz, (ed.), HTD, Vol. 100, ASME, New York, 13–24

Lage, J. L., Lim, J. S., Bejan, A. 1992. Natural convection with radiation in a cavity with open top end. *J. Heat Transfer*, **114**, 479–486

Lee, S. and Yovanovich, M. M. 1992. Linearization of natural convection from a vertical plate with arbitrary heat-flux distributions. *J. Electronic Packaging*, **114**, 909–916

Milanez, L. F. and Bergles, A. E. 1986. Studies on natural convection heat transfer from thermal sources on a vertical surface. *Proc. 8th International Heat Transfer Conference*, 1347–1352

Park, K. A. and Bergles, A. E. 1987. Natural convection heat transfer characteristics of simulated microelectronic chips. *J. Heat Transfer*, **109**, 90–96

Tewari, S. S. and Jaluria, Y. 1990. Mixed convection heat transfer from thermal sources mounted on horizontal and vertical surfaces. *J. Heat Transfer*, **112**, 975–987